SPHERAL SIMULATIONS OF THE DART SPACECRAFT IMPACT AT DIMORPHOS.

M. Bruck Syal[1], K. M. Kumamoto[1], J. M. Owen[1], J. M. Pearl[1], C. D. Raskin[1], E. B. Herbold[1], R. G. Kraus[1], A. M. Stickle[2], O.S. Barnouin[2], R.T. Daly[2], C.M. Ernst[2], M. Pajola[3], F. Tusberti[3], A. Lucchetti[3], N. Murdoch[4], C. Robin[4] , J. M. Sunshine[5], J. M. Trigo-Rodríguez[6], A. Zinzi[7], E. Dotto[7], V. Della Corte[7], E. Mazzotta Epifani[7], and the LICIACube Team https://www.ssdc.asi.it/liciacube/lcc_team.php. [1]Lawrence Livermore National Laboratory, Livermore CA, syal1@llnl.gov; [2]The Johns Hopkins University Applied Physics Laboratory, Laurel, MD; [3]INAF-OAPd, Padua, Italy; [4]ISAE-SUPAERO, Toulouse, France; [5]University of Maryland, College Park, MD; [6]CSIC-IEEC, Barcelona, Catalonia, Spain; [7]Agenzia Spaziale Italiano, Rome, Italy

Introduction: On September 26, 2022, NASA's DART mission successfully executed the first asteroid deflection experiment [1], when the spacecraft impacted the ~150-m asteroid Dimorphos, which was orbiting the ~760-m asteroid Didymos with a pre-impact period of 11 hours and 55 minutes. Post-impact, the orbital period was shortened to 11 hours and 23 minutes; Earth-based telescopes measured this change in orbital period to high precision [2]. DART delivered a total momentum impulse that exceeded the momentum of the spacecraft itself (m ~ 600 kg, v ~ 6.14 km/s), due to significant production of impact ejecta [3], much of which exceeded the escape velocity of Dimorphos (~5 cm/s).

Detailed images of the impact site (Fig. 1) were acquired by the Didymos Reconnaissance and Asteroid Camera for Opnav (DRACO) instrument [4], which enable accurate modeling of the shape and structure of Dimorphos for impact simulations [5,6]. Additionally, the Light Italian Cubesat for Imaging of Asteroids (LICIACube) [7] was released from the DART spacecraft 15 days before impact and captured flyby images of the cratering event (Fig. 2). These views provided supplementary information on the morphology of the crater ejecta, which can also be used to inform impact modeling choices and, ultimately, the inferred material properties for Dimorphos.

Fig. 1. Final full DRACO image of the DART impact site at Dimorphos, taken 1.818 seconds before the spacecraft's collision. Surface topography is included in Spheral simulations of the DART impact. Dimorphos north is to the upper right of the image. Credit: NASA/JHUAPL

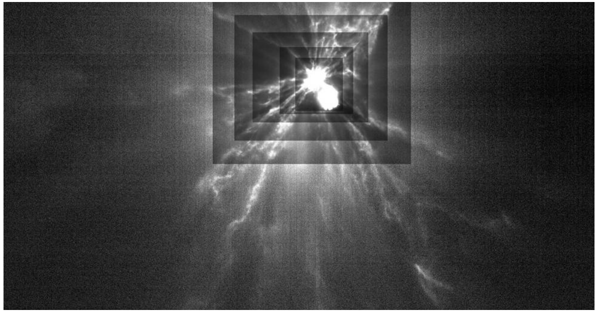

Fig. 2. LICIACube composite image of DART impact ejecta. Credit: ASI/NASA/JHUAPL

Here we report on initial three-dimensional simulations of the DART impact, which incorporate both the detailed shape and structure of Dimorphos and the engineering model of the DART spacecraft. The measured period change provides a critical constraint for the models, as the calculated momentum delivered from both the spacecraft and ejecta must be consistent with Dimorphos' altered trajectory. Although data analysis is ongoing, ejecta observations from both LICIACube and Earth-based telescopes can provide additional constraints, including: total ejecta mass, ejecta cone angle, ejecta ray morphology, boulder mobilization, and crater growth timescales.

Numerical Methods: Three-dimensional simulations are carried out in Spheral [8,9], an open source, Adaptive Smooth Particle Hydrodynamics (ASPH) code. Key features of the code, including accurate modeling of anisotropic strain fields through adaptive node sampling, benchmarked damage models, an array of built-in equations of state and constitutive models, and user-extendibility to new physics packages, make Spheral well-suited for simulating impulsive asteroid mitigation scenarios [10,11]. In preparation for the DART experiment, Spheral's capabilities have been extended to allow simulation of the full engineering CAD model of the DART spacecraft colliding with Dimorphos [12]. Additional pre-impact work included participation in an "Inverse Test," in which an ensemble of models explored a large parameter space, exploiting machine learning to efficiently cover a range of possible initial conditions [13]. The range of parameter combinations that produced results consistent with the period change measurement (solutions) provides intuition for tradeoffs in the inverse problem.

Projectile momentum and energy coupling, shock propagation, and crater excavation can all be affected by details of the target's topography and structure. In anticipation of a "rubble pile" type of structure, which has been observed at other Near-Earth Asteroids, rubble-pile node generators have been built into Spheral, for the purposes of more accurately modeling the impulsive deflection of asteroids (Fig. 3).

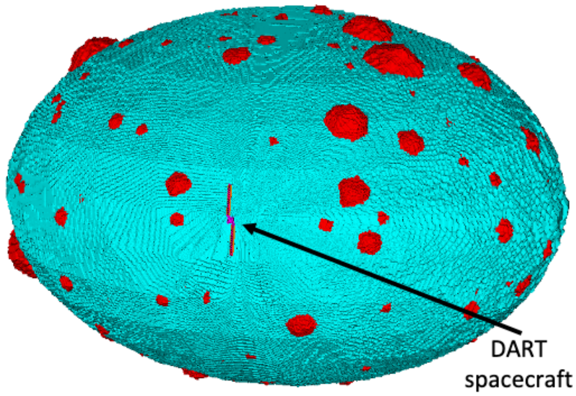

Fig. 3. Example of a randomized rubble pile structure, applied to the best-fit oblate spheroid for Dimorphos. Boulders are shown in red; matrix material in cyan.

Results: With the initial details of Dimorphos, the orbital period change, and crater ejecta properties in hand, hundreds of three-dimensional Spheral simulations have now been run, to begin narrowing in on the range of target properties consistent with available measurements. Fig. 4 shows a subset of machine-learning-driven simulations, many of which exceeded the targeted delta-v range. Over time, we expect a range of constitutive properties may be consistent with the system's period change, driven in large part by uncertainties in the bulk density of Dimorphos. For example, a low-strength and high-density target may receive the same total delta-v as a high-strength and low-density target.

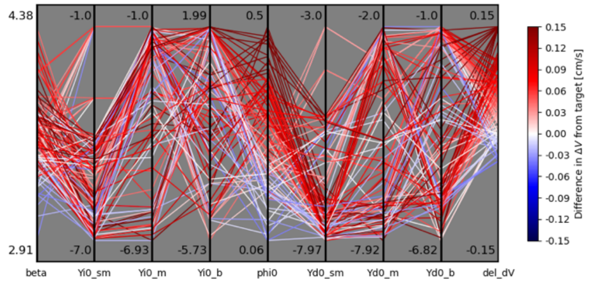

Fig. 4. Parallel coordinate plot for ensemble of 3-D DART models with different target properties. Red lines overshoot Dimorphos' measured delta-v; blue lines undershoot. To simplify the plot, we only show Yi (intact yield strength) and Yd (damaged yield strength) for each layer, as well as phi0 (bulk porosity).

In addition to these broad scans across possible material properties, which utilize random distributions of boulders, high-fidelity simulations of the impact are being carried out. These simulations include details of the observed boulder size-frequency distribution, the specific near-impact-site boulder field, and the spacecraft geometry. While simulations with either the spacecraft engineering model or a rubble-pile target have been carried out independently in the past, including both the detailed impactor and target geometry, together, can introduce new effects. Early work shows that the morphology of the ejecta cone produced on a rubble pile target is different for varying representations of the spacecraft (Fig 5).

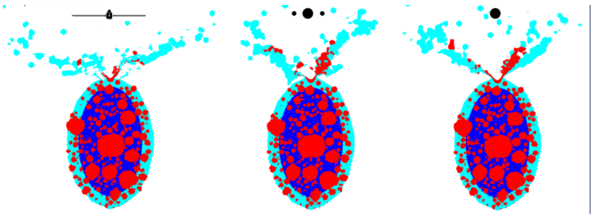

Fig. 5. Impactors are often simplified into idealized shapes, such as a sphere (right), or three-sphere (center) representation. However, when considering the interplay of spacecraft geometry with a local boulder distribution, some details of the ejecta morphology may depend upon using a full engineering model for the spacecraft (left). Dimorphos models shown here include a rubble-pile distribution of boulder, and two distinct layers of matrix material (to allow free variation of properties in each layer; the uppermost layer is assumed to be weaker). Impactors are representative and not to scale.

References: [1] Rivkin, A. S. et al. 2022 *Planet. Sci. J.* **2** 173. [2] Thomas, C. A. et al. 2023 (submitted). [3] Cheng, A. F. et al. 2023 (submitted). [4] Fletcher, Z. J. et al. 2018 Proc. SPIE 10698. [5] Daly, R. T. et al. 2022 *Planet. Sci. J.* **3** 207. [6] Daly, R. T. et al. 2023 (submitted). [7] Dotto E. et al. 2021 *PSS* **199** 105185. [8] Owen, J. M. et al. 1998. *Astrophys. J. Suppl. S.* **116**, 155–209. [9] Owen, J. M. 2010. 5th International SPHERIC SPH Workshop. [10] Owen, J. M. 2014. *Int. J. Numer. Meth. Fl.* **75**, 749-774. [11] Owen, J. M. 2015. *Procedia Engineering* **103**, 466–474. [12] Owen, J. M. et al. 2022 *Planet Sci. J.* **3** 218. [13] Kumamoto, K. M. et al. 2022 *Planet. Sci. J.* **3** 237.

The work performed by LLNL is under the auspices of the U.S. Department of Energy by Lawrence Livermore National Laboratory under Contract DE-AC52-07NA27344. LLNL-ABS- 843778